OPTICAL MODEL POTENTIAL SEARCH FOR NEUTRON- AND PROTON-INDUCED REACTIONS OF ^{12}C, ^{16}O, ^{27}AL, ^{56}FE, ^{90}ZR AND ^{208}PB UP TO 250 MEV

Young-Ouk LEE and Jonghwa CHANG
Nuclear Data Evaluation Lab., KAERI
P.O Box 105 Yusung, Taejon, Korea
yolee@lui.kaeri.re.kr ; jhchang@kaeri.re.kr

Tokio FUKAHORI and Satoshi CHIBA
Nuclear Data Center, JAERI
Tokai-mura, Naka-gun, Ibaraki-ken, 319-1195 Japan
fukahori@cracker.tokai.jaeri.go.jp ; chiba@hadron31.tokai.jaeri.go.jp

February 25, 2000

ABSTRACT

Recent new applications, such as the accelerator-driven transmutation of nuclear waste and radiation transport simulations of cancer radiotherapy require evaluated nuclear data on neutron- and proton-induced reactions up to a few GeV. The optical model provides the basis for theoretical evaluations of nuclear cross sections for such applications up to a few hundreds MeV of incident nucleon. In order to perform nuclear data evaluation without unphysical discontinuities, optical models should cover the whole mass and energy range of interest continuously. In this work, a set of optical model parameters were searched with energy dependent potential forms which incorporate the effects of dispersion relationship for neutrons and protons up to 250 MeV on ^{12}C, ^{16}O, ^{27}Al, ^{56}Fe, ^{90}Zr and ^{208}Pb. Calculated cross sections with the resulting optimum optical model parameters described a wide range of measured data fairly well.

1. INTRODUCTION

Nuclear data for conventional fission reactors and fusion devices mainly consist of neutron-induced cross sections in energy below 20 MeV. However, recent new applications, such as

radiation transport simulations of cancer radiotherapy and the accelerator-driven transmutation of nuclear wastes require evaluated nuclear data on neutron- and proton-induced reactions above 20 MeV and up to a few GeV.

The optical model provides the basis for theoretical evaluations of nuclear cross sections that are used in providing nuclear data for applications. In addition to offering a convenient means for calculations of reaction, shape elastic, and (neutron) total cross sections, optical model potentials are widely used in quantum-mechanical preequilibrium and direct-reaction theory calculation. But the most important role of optical model anaysis is to supply particle transmission coefficients for Hauser-Feshbach statistical theory anayses used in nuclear data evaluations.

In order to perform nuclear data evaluation without unphysical discontinuities, optical models should cover the whole energy range of interest continuously. Currently many optical model segments are available for nuclear date evaluations, but most of them have been derived over very limited energy and mass regions. In the Reference Input Parameter Library (RIPL) published by the IAEA,[1] only the Koning, Wijk and Delaroche[2] potential for neutron reactions of Zr-90 has a truly broad energy range of validity. Recently Chadwick *et al.*[3] applied Madland's global medium energy optical model[4] over wide mass and energy region. It is reported that this global potential gives a good description of measured neutron and proton cross sections for some isotopes up to 160 MeV. Also mentioned is that the Madland's global optical potential cannot reproduce all the measured data in more detail. To supplement the Madland's global optical model, they adopted the energy dependent potential forms[5] which incorporate effects of the dispersion relationship proposed by Delaroche *et al.* for some isotopes, giving better agreement with the measurements. Lee *et al.*[6] also adopted the same potential form in evaluating neutron and proton cross sections of Al-27 up to 250 MeV successfully. Present study is part of the ground work to establish a global optical potential form having effects of dispersion relationship over a wide mass range and up to 250 MeV. Here, the energy dependent optical model parameters of Delaroche type OMP were searched up to 250 MeV for the isotopes of interest: ^{12}C, ^{16}O, ^{27}Al, ^{56}Fe, ^{90}Zr and ^{208}Pb.

Section 2 briefly describes the adopted potential form and parameters. Section 3 deals with reference measurements and section 4 with search procedures. Final section summarizes the results and discussion.

2. POTENTIAL FORM

The potential form factor was chosen to be of Woods-Saxon form for V_r and W_v, derivative Woods-Saxon for W_d and Thomas-Fermi form for spin-orbit parts as

$$\begin{aligned} U(r) &= -V_r f_v(r) - iW_v\ f_w(r) + 4i\ a_{wd}\ W_d\ \frac{df_{wd}(r)}{dr} \\ &\quad -\frac{1}{r}\left(\frac{\hbar}{m_\pi c}\right)^2 \left(V_{so}\frac{d}{dr}f_{vso}(r) + iW_{so}\frac{d}{dr}f_{wso}(r)\right)\ \boldsymbol{l}\cdot\boldsymbol{s}\ + V_{Coul}. \end{aligned} \tag{1}$$

where m_π is the mass of the pion and the form factors f_i are of the standard Woods-Saxon shape :

$$f_i(r) \equiv \frac{1}{1+exp((r-r_i A^{1/3})/a_i)}, \quad i = v, w, wd, vso, wso \tag{2}$$

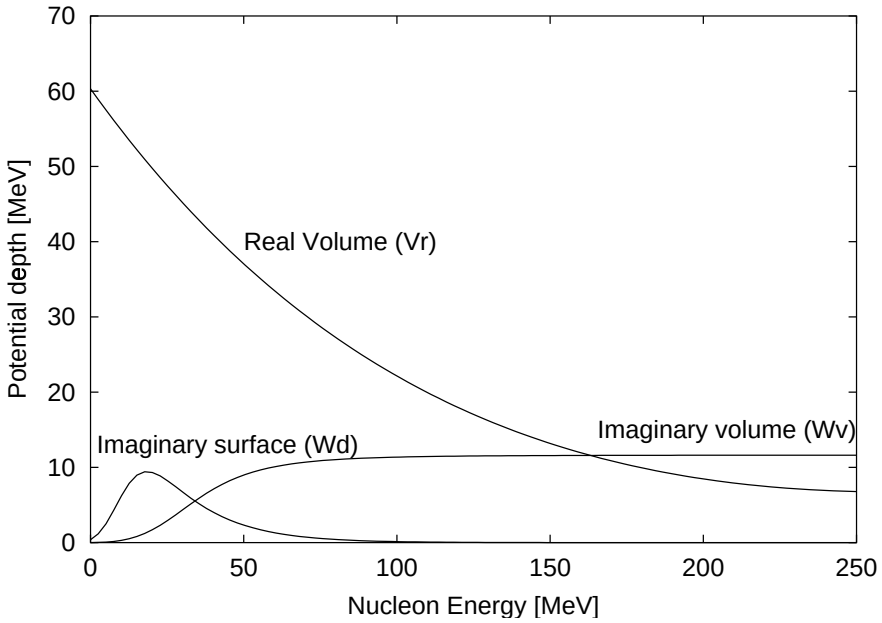

Figure 1: The volume potential depths of real volume, imaginary volume and imaginary surface as a function of neutron and proton energy

Here, a_i is the diffuseness parameter, and A the target mass number.

Figure 1 presents the general shapes of the potential depths of real volume (V_r), volume absorptive (W_v) and surface absorptive (W_d) adopted in this work to incorporate effects of the dispersion relationship. $V_r(E)$ decreases exponentially down to a few MeV for incident nucleon energies around 250 MeV. $W_d(E)$ increases to reach a plateau at around 10 MeV and then decreases smoothly with energy. W_v(E) is negligible for incident energies below 10 MeV, then increases to reach a plateau at around 70 MeV.

These shapes have following functional forms:

$$\begin{aligned} V_r(E) &= V_0 e^{-\lambda_{vr}(E-E_f)} + V_1 + V_2 E \\ W_v(E) &= W_{v0} \frac{(E-E_f)^4}{(E-E_f)^4 + W_{v1}^4} \\ W_d(E) &= W_{d0} e^{-\lambda_{wd}(E-E_f)} \frac{(E-E_f)^4}{(E-E_f)^4 + W_{d1}^4}, \\ r_i(E) &= r_{i0} + r_{i1} E \\ a_i(E) &= a_{i0} + a_{i1} E \end{aligned} \tag{3}$$

where the Fermi energy E_f for neutrons and protons is given by

$$\begin{aligned} \text{neutron} \quad E_f(Z,A) &= -\frac{1}{2}[S_n(Z,A) + S_n(Z,A+1)] \\ \text{proton} \quad E_f(Z,A) &= -\frac{1}{2}[S_p(Z,A) + S_p(Z+1,A+1)] \end{aligned} \tag{4}$$

The geometry factor of W_v is assumed to be the same as that of V_r as

$$r_v(E) = r_{wv}(E) \neq r_{wd}(E)$$
$$a_v(E) = a_{wv}(E) \neq a_{wd}(E) \quad (5)$$

Above leaves 17 adjustable parameters for the enrgy range 0 - 250 MeV of incident neutron and proton.

3. REFERENCE MEASUREMENTS

The role of experimental data for the nuclear data evaluation is important; it guides modelling of nuclear reactions, but also validate the models and parameters. From this view point, it is desirable that the reference experimental data span over a certain number of nuclei, reactions and incident energies. For the reference data of neutron and proton induced reactions up to 250 MeV region, the EXFOR[7] database was extensively surveyed, analyzed, and Table 1 lists the selected reference maeasurements. n

4. PARAMETER SEARCH

The best sets of OMP were determined by adjusting the 17 adjustable coefficients defined in eq. (3) and (5) with the use of ECISPLOT,[66] an interactive optical parameter searcher with the simulated annealing algorithm, developed by one of the authors. This is an X-Window based software system incorporated into the nuclear reaction code ECIS-96.[67] In ECISPLOT, the potential parameters are adjusted interactively based on an eye-guide, then the final parameter set is searched automatically by the simulated annealing algorithm to have minimum χ^2. During the ECISPLOT operation, smooth-varying potential depths and form factors could be collected with respect to the incident energies. With these points, rough fittings and interactive tuning were applied to get the initial 17 coefficients. Finally, a simulated annealing algorithm was applied to get the best optimum coefficient set within the ranges for each coefficient as listed in table 1.

The quantity χ^2 in this study is defined by

$$\chi^2 = \frac{1}{N+M}\left[\sum_{i=1}^{N}\frac{1}{K_i}\sum_{j=1}^{K_i}\left(\frac{d\sigma_{ij}/d\Omega_{calc} - d\sigma_{ij}/d\Omega_{exp}}{\Delta\sigma_{ij}/d\Omega_{exp}}\right)^2 + \sum_{i=1}^{M}\left(\frac{\sigma_{tot_{cal_i}} - \sigma_{tot_{exp_i}}}{\Delta\sigma_{tot_{exp_i}}}\right)^2\right] \quad (6)$$

where N is the number of experimental scattering data sets, K_i is the number of angular points in each data set, M is the number of energies for which experimental neutron total cross section or proton reaction cross sedction is involved.

Simulated Annealing(SA)[68] is a global optimization method that distinguishes between different local optima. Starting from an initial point, the algorithm takes a step and the function is evaluated. When minimizing a function, any downhill step (decreasing the χ^2) is accepted and the process repeats from this new point. An uphill step (increasing the χ^2) may be accepted. Thus, the process can escape from local optima. This uphill decision is made by the Metropolis criteria. As the optimization process proceeds, the

Table 1: Reference measurements for neutron induced reactions

Reaction	Cross Section	Principal Author	Energy Range [MeV]
n+^{12}C	total cross section	Auman[8]	24-60
		Lamaze[9]	2-40
		Peterson[10]	61-106
	elastic angular distribution	Meigooni[11]	20.8, 26.0
		Niizeki[12]	35.0
		Winfield[13]	40.3
		Hjort[14]	65.0
		Salmon[15]	96.0
		Zyl[16]	136.0
n+^{16}O	total cross section	Foster-jr[17]	2-14
		Alphonce[18]	109-163
	elastic angular distribution	Islam[19]	18.0, 20.0, 22.0, 26.0
n+^{27}Al	total cross section	Auman[8]	30-60
		Bubb[20]	21-44
		Measday[21]	88-150
		Franz[22]	160-575
	elastic angular distribution	Petler[23]	18.0, 20.0, 25.0, 26.0
		Olsson[24]	21.6
		Petler[23]	22.0
		Stuart[25]	24.0
		Bratenahl[26]	84.0
		Salmon[15]	96.0
		Zyl[16]	136.0
n+^{56}Fe	total cross section	Ragent[27]	36-19
		Albergotti[28]	12-14
		Zanelli[29]	35-50
	elastic angular distribution	Smith[30]	4.5
		El-kadi[31]	8.0
		Mellema[32]	11.0, 20.0, 26.0
		Pedroni[33]	16.9
		Hjort[14]	65.0
n+^{90}Zr	total cross section	Finlay[34]	
		Tanaka[35]	5.9, 7.0
		Wang[36]	8.0, 10.0, 24.0
		Bainum[37]	11.0
		Clarke[38]	14.1
n+^{208}Pb	total cross section	Finlay[34]	5-600
	elastic angular distribution	Rapaport[39]	11.0
		Finlay[40]	20.0, 24.0
		Vito[41]	30.3, 40.0
		Hjort[14]	65.0
		Salmon[15]	96.0
		Zyl[16]	136.0

Table 2: Reference measurements for proton induced reactions

Reaction	Cross Section	Principal Author	Energy Range [MeV]
p+^{12}C	reaction cross section	Mcgill[42]	23-48
		Kirkby[43]	99.7
		Pollock[44]	16
	elastic angular distribution	Ridley[45]	30.3
		Ohnuma[46]	35.2
		Fannon[47]	49.5
p+^{16}O	reaction cross section	Carlson[48]	19-48
	elastic angular distribution	Cameron[49]	23.4
		Ohnuma[50]	35.0
		Fannon[47]	49.5
		Sakaguchi[51]	65.0
p+^{27}Al	reaction cross section	Menet[52]	40-61
		Renberg[53]	234-554
		Mcgill[42]	25-46
		Kirkby[43]	99.7
	elastic angular distribution	Dayton[54]	17.0
		Bertrand[55]	28.8, 61.7
		Taylor[56]	142.0
p+^{56}Fe	reaction cross section	Mccamis[57]	21-48
		Menet[52]	40-61
		Renberg[53]	234-554
		Kirkby[43]	98.7
	elastic angular distribution	Dayton[54]	17.0
		Eccles[58]	19.1
		Ridley[45]	30.3
		Bertrand[55]	61.5
		Comparat[59]	156.0
p+^{90}Zr	reaction cross section	Menet[52]	40-61
	elastic angular distribution	Makofske[60]	16.0
		Blumberg[61]	40.0
		Sakaguchi[51]	65.0
		Comparat[59]	156.0
		Nadasen[62]	180.0
		Hagberg[63]	185.0
p+^{208}Pb	reaction cross section	Renberg[53]	234-554
		Carlson[48]	21-48
		Kirkby[43]	99.2
	elastic angular distribution	Oers[64]	21.0, 24.1 26.3, 30.0, 35.0
		Fulmer[65]	45.0

Table 3: Range of optical model parameters for incident neutron and proton energies up to 250 MeV

	lower bound	upper bound
V_r (MeV)	0.0	60.0
W_v (MeV)	0.0	15.0
W_d (MeV)	0.0	10.0
r_v, r_w,r_{wd} (fm)	1.0	1.4
a_v,a_w, a_{wd} (fm)	0.4	1.0

length of the steps declines and the algorithm closes in on th local optimum. Since the algorithm makes very few assumptions regarding the function to be optimized, it is quite robust with respect to the non-quadratic surfaces. The actual procedure of SA operation in ECISPLOT is as follows:

- Start with the initial coefficients within their upper and lower bounds defined in table 1, and initial sampling range as half of the bounds. Estimate χ^2 with the initial set of coefficients.
- For the next step, randomly choose a trial point within the sampling range and χ^2 is evaluated at this point.
- This χ^2 is compared to the previous one. All downhill moves are accepted and the algorithm continues from that trial point.
- Uphill moves may be accepted; the decision is made by the Metropolis criteria with a random variable z.

$$\exp\left(\frac{\chi_k^2 - \chi_{k+1}^2}{T}\right) > z \tag{7}$$

  It uses T(temperature) and the size of the uphill move in a probabalistic manner. The smaller the T and size of the uphill move are, the more likely it is that the move will be accepted.
- If the trial is accepted, the algorithm moves on from that point. If it is rejected, another point is chosen instead of the trial point.
- Sampling ranges for each parameter are periodically adjusted so that half of all function evaluations in that direction are accepted.
- A fall in T is imposed upon the system with the RT variable by

$$T_{m+1} = \mathrm{RT} \cdot T_m \tag{8}$$

  where m is the mth iteration with the same T. Thus, as T declines, uphill moves are less likely to be accepted and the percentage of rejections rise. Thus as T declines, the sampling range becomes narrow and focuses upon the most promising area for optimization.

- The termination criteria for the search in ECISPLOT is set if the last four χ^2's from the last four different T's differ from the current χ^2 by less than the user-defined tolerance(EPS) and the current χ^2 at the current T differs from the current optimal χ^2 by less than EPS.

5. RESULTS AND DISCUSSIONS

A set of optical model parameters were optimized by searching 17 adjustable coefficients defined in eq. (3) and (5), with the SA method of ECISPLOT. Table 1 lists the optimized coefficients which describe the reference experimental data with converged χ^2 for neutrons and protons. The total (for neutron) and reaction (for proton) cross sections, and elastic angular distributions from the optimized optical model parameters are compared in Figs. 2 -7 with the reference measurements, as well as other data not adopted as references. The optimized optical model parameters give overall agreement with most of the experimental data over the entire energy range for both incident neutrons and protons. It is also noted that for incident energies below around 10 MeV, the optical model cross sections describes the smoothed average of the resonance structures well.

The resulting optical model parameters supply not only the reaction, shape elastic, and neutron total cross sections, but also the neutron and proton transmission coefficients for the Hauser-Feshbach statistical analyses used in nuclear data evaluations. Based on the results of present work, appropriate systematics will be tried to establish a global optical potential form having effects of dispersion relationship, covering wider mass and energy range.

ACKNOWLEDGEMENTS

This work was performed under the auspices of the Korea Ministry of Science and Technology as one of the long-term nuclear R&D programs.

Table 4: Neutron and proton optical potential parameters up to 250 MeV

	n+^{12}C	n+^{16}O	n+^{27}Al	n+^{56}Fe	n+^{90}Zr	n+^{208}Pb
E_f (MeV)	-11.8341	-9.9036	-10.3900	-9.4222	-9.5827	-5.6524
V_0 (MeV)	105.1117	105.3141	103.4468	104.3836	105.7053	104.4845
λ_{vr} MeV^{-1})	0.0056	0.0054	0.0050	0.0051	0.0054	0.0053
V_1 (MeV)	-45.7867	-46.1060	-46.4998	-45.7773	-50.6796	-52.2968
V_2 (MeV^{-1})	0.1112	0.1326	0.1064	0.1082	0.1598	0.1440
r_{v0} (fm)	1.1191	1.1321	1.1793	1.1689	1.2237	1.2207
r_{v1} (fm/MeV)	0.0009	0.0006	0.0001	0.0005	0.0002	0.0004
a_{v0} (fm)	0.6603	0.6684	0.6020	0.6498	0.5402	0.5868
a_{vl} (fm/MeV)	0.0010	0.0005	0.0020	0.0001	0.0002	-0.0009
W_{v0} (MeV)	8.2824	8.5000	8.5000	8.4891	7.3034	8.4383
W_{v1} (MeV)	39.1468	43.1924	30.0051	42.9775	35.2851	44.2294
W_{d0} (MeV)	35.7590	32.0086	17.9433	41.6125	28.9006	20.7907
λ_{wd} (MeV^{-1})	0.0532	0.0494	0.0522	0.0581	0.0640	0.0410
W_{d1} (MeV)	20.0888	22.9954	10.3142	19.7508	21.0470	15.3310
r_{wd0} (fm)	1.2692	1.2011	1.2785	1.2081	1.1668	1.2445
r_{wd1} (fm/MeV)	0.0069	0.0035	0.0000	0.0007	0.0005	-0.0009
a_{wd0} (fm)	0.3148	0.5622	0.5989	0.6250	0.9276	0.6463
a_{wd1} (fm/MeV)	-0.0007	-0.0007	-0.0009	-0.0009	0.0001	0.0010

	p+^{12}C	p+^{16}O	p+^{27}Al	p+^{56}Fe	p+^{90}Zr	p+^{208}Pb
E_f (MeV)	-8.9504	-6.3639	-9.9284	-8.1062	-6.7575	-5.9055
V_0 (MeV)	107.0000	104.4750	105.0000	106.3129	106.5222	108.4518
λ_{vr} MeV^{-1})	0.0059	0.0054	0.0051	0.0055	0.0067	0.0078
V_1 (MeV)	-45.6436	-45.6405	-45.3829	-45.7034	-41.4619	-34.5341
V_2 (MeV^{-1})	0.1004	0.1156	0.1034	0.1112	0.1176	0.1389
r_{v0} (fm)	1.1251	1.1582	1.1680	1.2023	1.1918	1.2019
r_{v1} (fm/MeV)	0.0000	0.0007	0.0000	0.0003	0.0004	0.0002
a_{v0} (fm)	0.5775	0.6147	0.6481	0.6282	0.6799	0.6420
a_{vl} (fm/MeV)	0.0012	0.0018	0.0023	0.0007	-0.0005	0.0000
W_{v0} (MeV)	10.8366	7.7972	8.5965	10.7583	11.6313	16.4091
W_{v1} (MeV)	50.1011	39.4362	29.6722	48.9014	41.8397	47.0136
W_{d0} (MeV)	36.3452	99.5854	20.6320	53.0375	63.9901	18.6886
λ_{wd} (MeV^{-1})	0.0583	0.0624	0.0439	0.0625	0.0580	0.0404
W_{d1} (MeV)	28.9709	27.5714	19.9513	14.7125	21.9205	10.2981
r_{wd0} (fm)	1.1375	1.2433	1.4221	1.2428	1.1978	1.2566
r_{wd1} (fm/MeV)	0.0085	0.0024	0.0000	0.0036	-0.0000	-0.0008
a_{wd0} (fm)	0.5887	0.3264	0.3460	0.5906	0.6088	0.9525
a_{wd1} (fm/MeV)	0.0004	-0.0001	0.0007	-0.0007	-0.0007	-0.0009

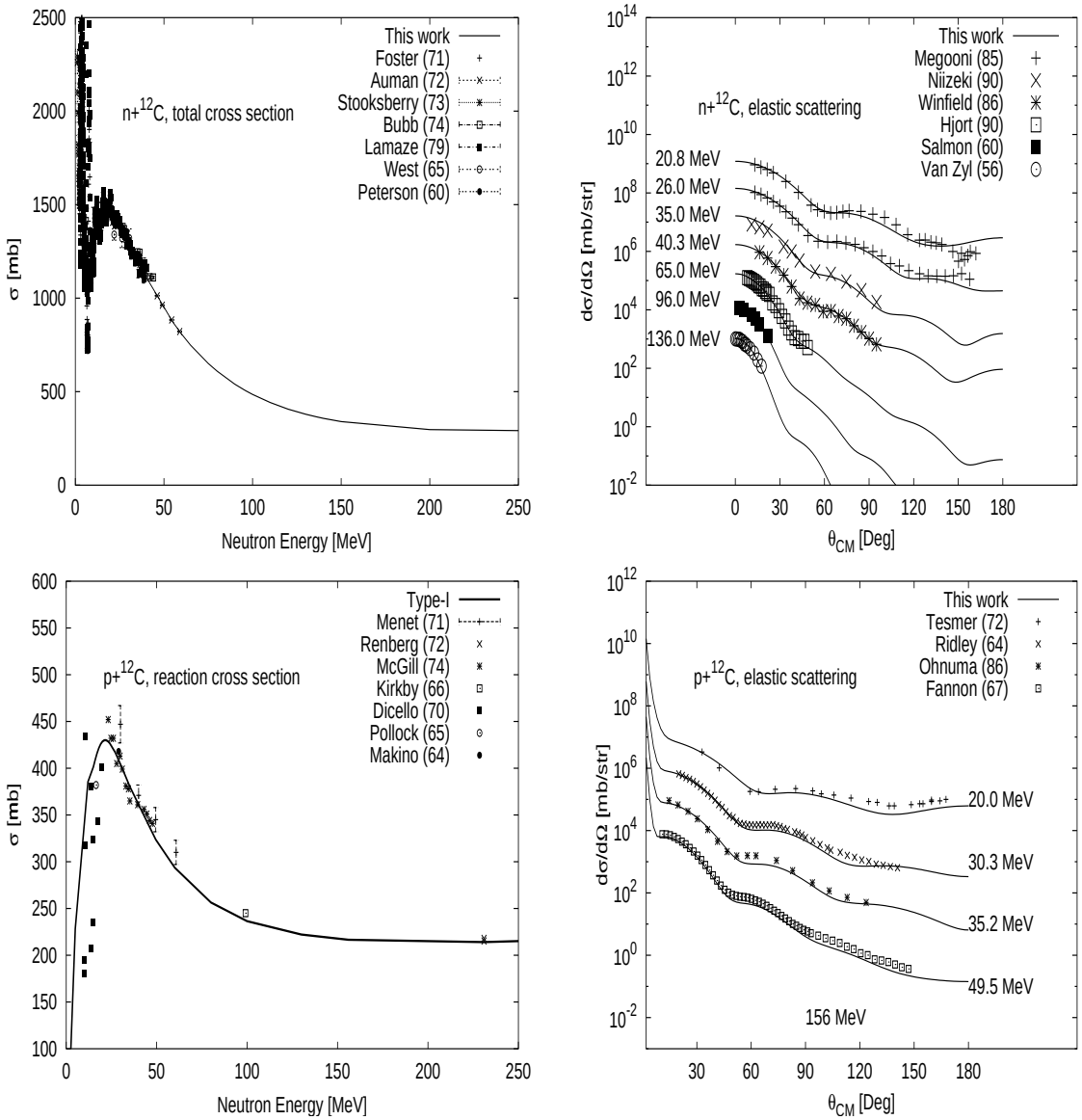

Figure 2: Total, reaction cross section and elastic angular distbution for n,p + ^{12}C reactions

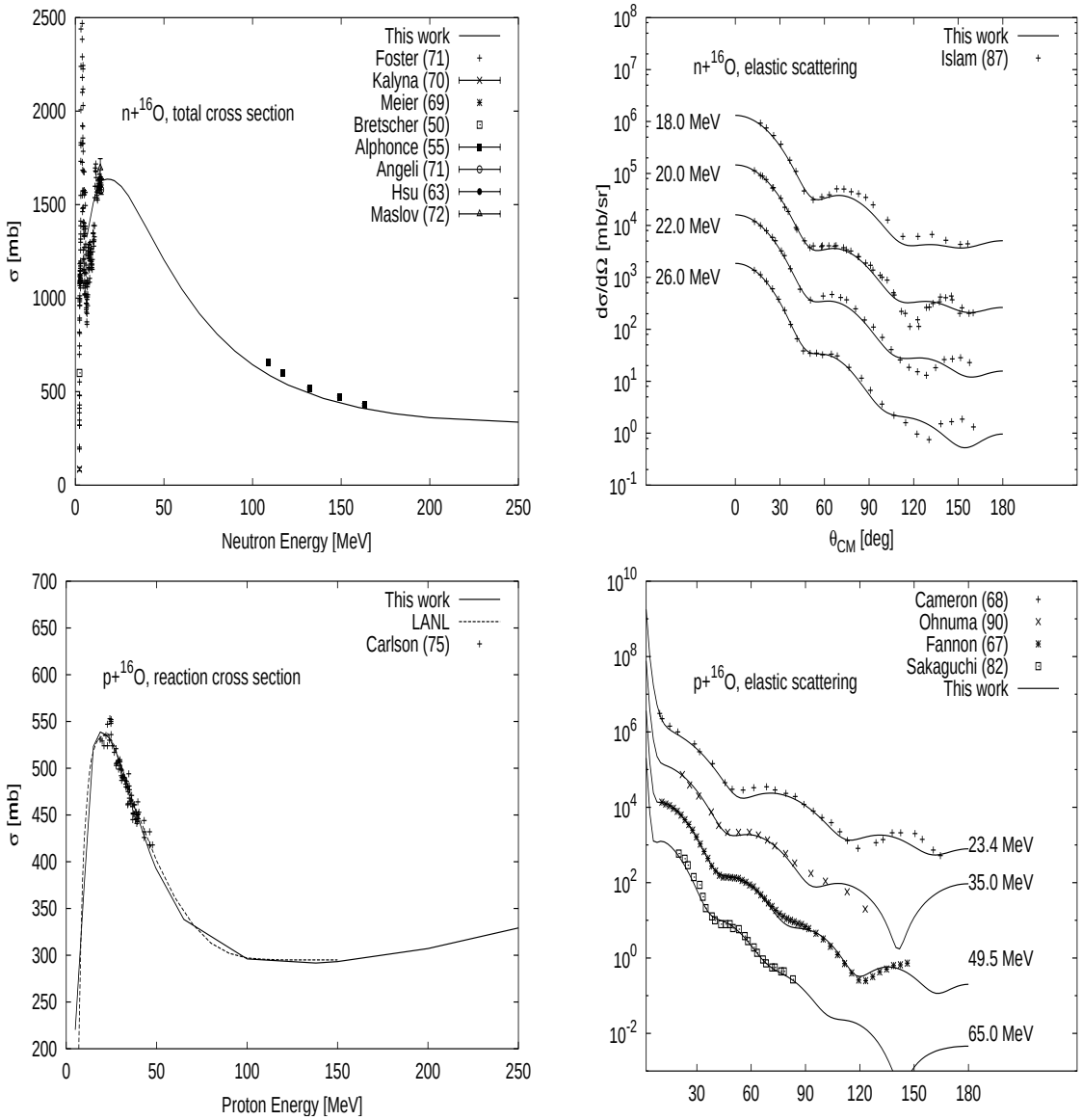

Figure 3: Total, reaction cross section and elastic angular distbution for n,p + ^{16}O reactions

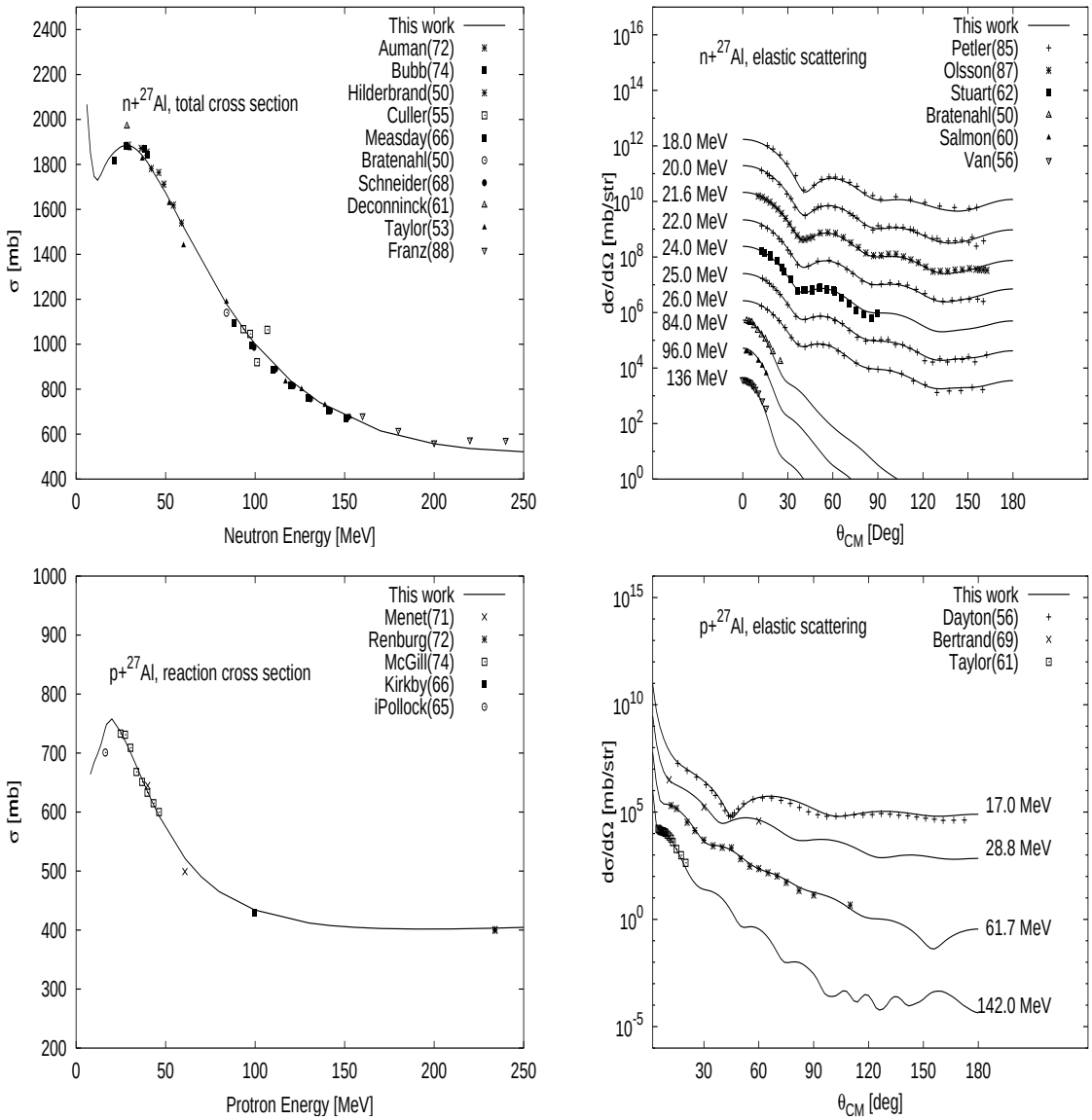

Figure 4: Total, reaction cross section and elastic angular distbution for n,p + ^{27}Al reactions

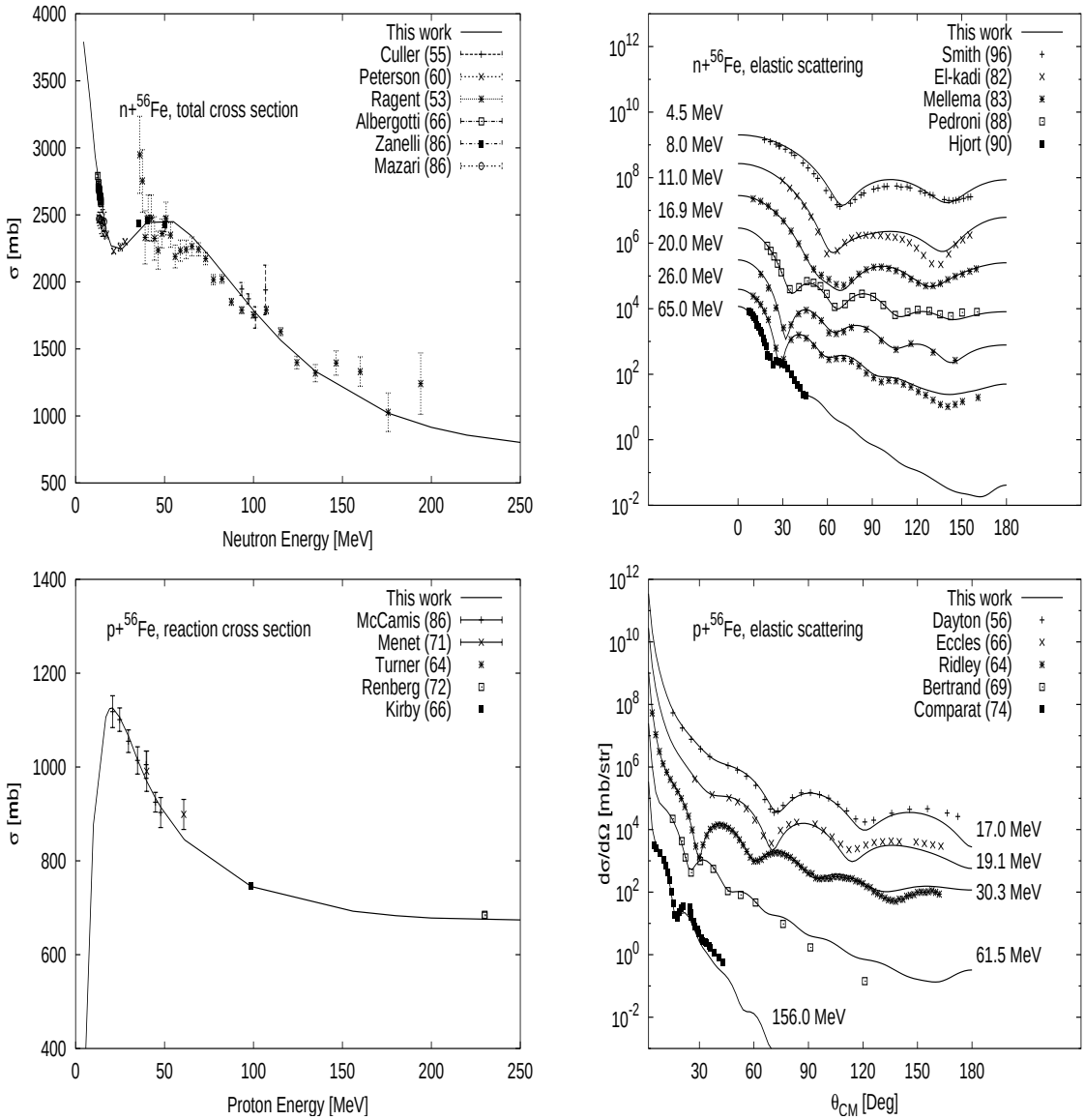

Figure 5: Total, reaction cross section and elastic angular distbution for n,p + ^{56}Fe reactions

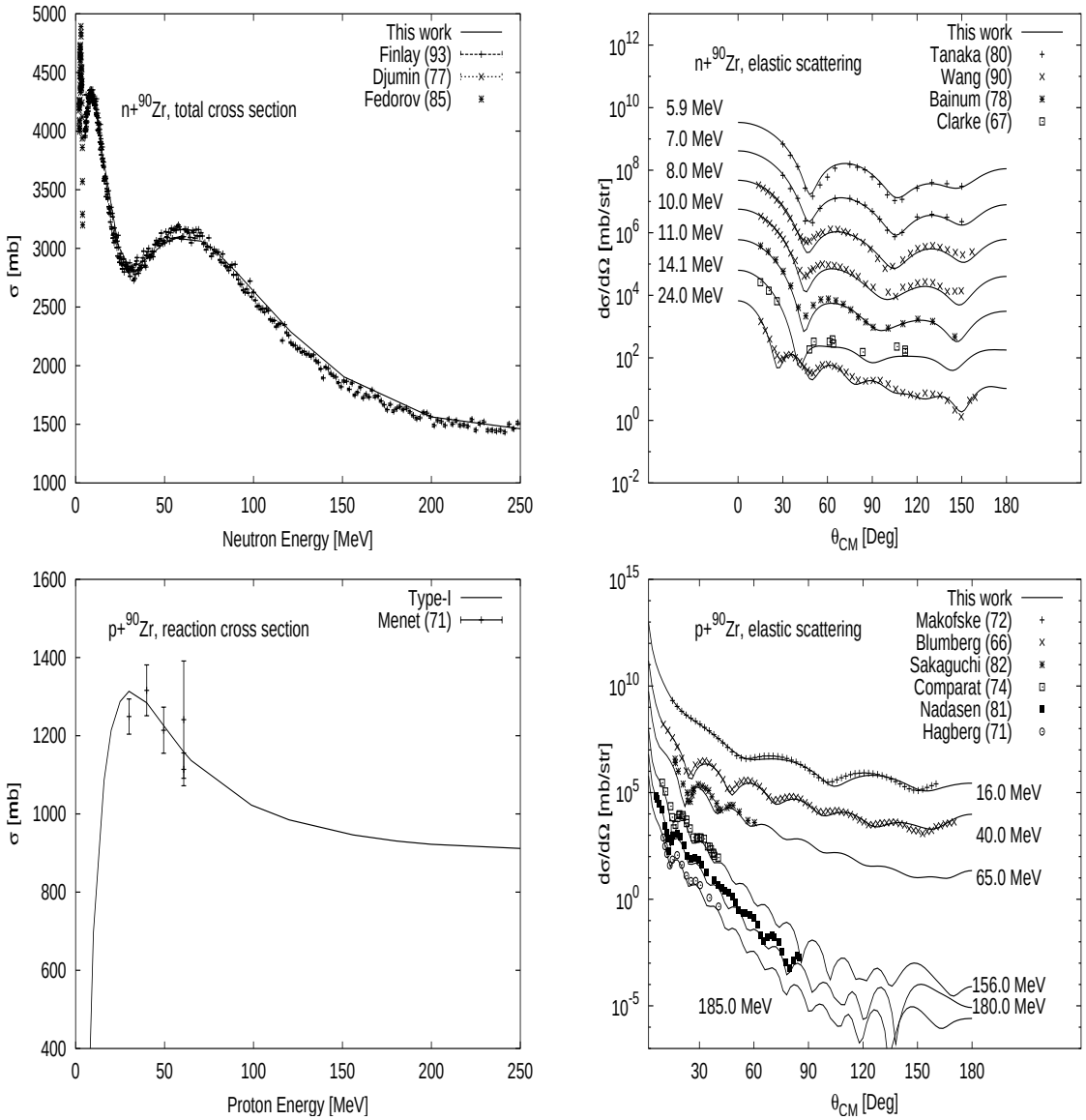

Figure 6: Total, reaction cross section and elastic angular distbution for n,p + ^{90}Zr reactions

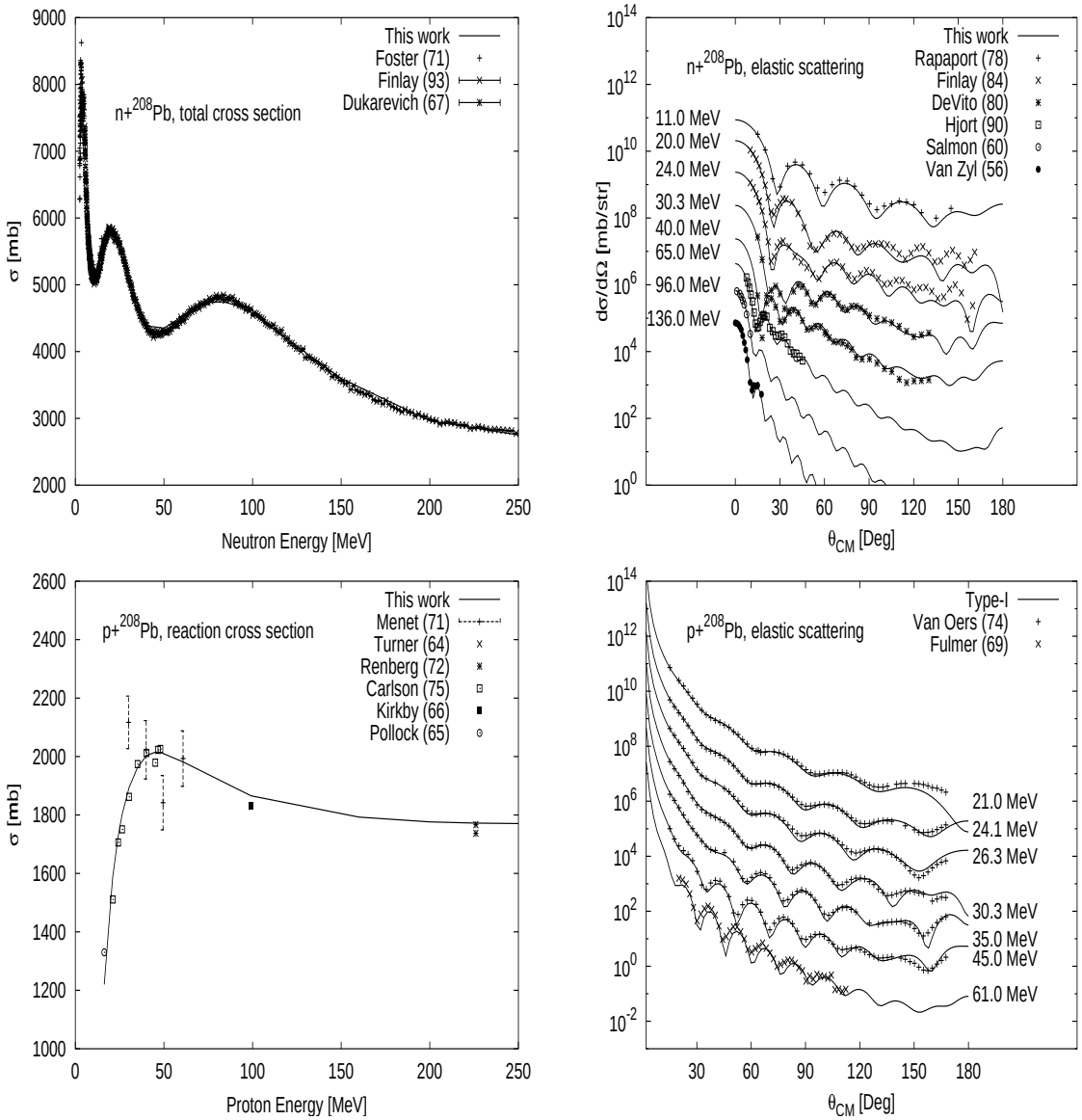

Figure 7: Total, reaction cross section and elastic angular distbution for n, p + ^{208}Pb reactions

REFERENCES

1. P. G. Young, "Ch4: Optical Model Parameters," Tech. Rep. IAEA TECDOC-1034, International Atomic Energy Agency, Vienna, Austria (1998).

2. A. J. Koning, J. P. Delaroche, and O. Bersillon, "Neutron and proton data files up to 150 MeV for 54Fe, 56Fe, 58Ni and 60Ni," Tech. Rep. ECN-RX-97-047, Netherlands Energy Research Foundation ECN, Petten, The Netherlands (1997).

3. M. Chadwick and et al., "Cross Section Evaluations to 150 MeV for Accelerator-Driven Systems and Implementation in MCNPX," *Nucl. Sci. Eng.*, vol. 131, p. 293 (1999).

4. D. G. Madland, "Recent Results in the Development of a Global Medium-Energy Nucleon-Nucleus Optical Model Potential," in *Proc. of a Specialists Meeting on Preequilibrium Reactions* (B. Strohmaier, ed.), no. NEANDC-245, (Paris, France), pp. 103–116, Semmering, Austria, 1988, OECD/NEA (1988).

5. J. Delaroche, Y. Wang, and J. Rapaport *Phys. Rev. C*, vol. 39, p. 391 (1989).

6. Y. Lee, T. Fukahori, J. Chang, and C. S., "Evaluation of Neutron- and Proton-induced Cross Section of Al-27 up to 2 GeV," in *Proc. of the 1998 Symposium on Nuclear Data, Nov. 19-20, 1998, JAERI, Tokai, Japan*, no. JAERI-Conf 99-002, p. 246 (1999).

7. OECD/NEA (Data Bank, WWW address: http://www.nea.fr).

8. M. Auman, F. Brady, J. Jungerman, W. Knox, M. Mcgie, and T. Montgomery, "Neutron total cross sections of the light elements in the energy range 24-60MeV," *Phys. Rev. C*, vol. 5 (1972). EXFOR 10230(720111C).

9. G. Lamaze, J. Kellie, and R. Schwartz, "Total cross section measurements of Li-6,Li-7 and C-12 from 3 to 40 MeV," in *Conf. On Nucl. Cross Sections F. Techn., Knoxville 1979* (1979). EXFOR 10888(790821C).

10. J. Peterson, A. Bratenahl, and J. Stoering, "Neutron total cross sections in the 17- to 29-MeV region," *Phys. Rev.*, vol. 120 (1960). EXFOR 11108(760924T).

11. A. Meigooni, R. Finlay, J. Petler, and J. Delaroche, "Nucleon-induced excitation of collective bands in 12C," *Nucl. Phys. A*, vol. 445 (1985). EXFOR 12944(870107C).

12. T. Niizeki, H. Orihara, K. Ishii, K. Maeda, M. Kabasawa, Y. Takahashi, and K. Miura, "Facilities for neutron induced experiments at the tohoku university cyclotron," *Nucl. Instrum. Methods In Phys. Res.,section A*, vol. 287 (1990). EXFOR 22167(910118C).

13. J. Winfield, S. Austin, R. Vito, U. Berg, Z. Chen, and W. Sterrenburg, "Measurements of elastic neutron scattering from 12C and 32S at 30.3 and 40.3 MeV. limits on charge symmetry breaking in the nuclear mean field," *Phys. Rev. C*, vol. 33 (1986). EXFOR 12871(860602C).

14. E. Hjort, *Elastic and inelastic neutron scattering at 65 MeV.* PhD thesis (1990). EXFOR 13510(910823C).

15. G. Salmon, "The elastic scattering of 96 MeV neutrons by nuclei," *Nucl. Phys.*, vol. 21 (1960). EXFOR 21123(790924C).

16. C. Zyl, R. Voss, and R. Wilson, "The elastic scattering of 136 MeV neutrons by nuclei," *Phil. Mag.*, vol. 1 (1956). EXFOR 21374(800213T).

17. D. Foster-jr and D. Glasgow, "Neutron total cross sections, 2.5 - 15 MeV. I. experimental," *Phys. Rev. C*, vol. 3 (1971). EXFOR 10047(730815C).

18. R. Alphonce, A. Johansson, A. Taylor, and G. Tibell, "Neutron attenuation measurements in heavy and light water at energies between 109 and 169 MeV," *Phil. Mag.*, vol. 46 (1955). EXFOR 21789(820814C).

19. M. Islam, R. Finlay, and J. Peter, "Elastic and inelastic scattering of nucleons from 16O," *Nucl. Phys. A*, vol. 464 (1987). EXFOR 13194(901008C).

20. I. Bubb, S. Bunker, M. Jain, J. Leonard, A. Ilwain, K. Roulston, K. Standing, D. Wells, and B. Whitmore, "Neutron total cross sections between 20 and 45 MeV," *Can. J. Phys.*, vol. 52 (1974). EXFOR 10379(740530C).

21. D. Measday and J. Palmieri, "Neutron total cross sections in the energy range 80 to 150 MeV," *Nucl. Phys.*, vol. 85 (1966). EXFOR 11151(760924T).

22. J. Franz, H. Grotz, L. Lehmann, E. Roessle, H. Schmitt, and L. Schmitt, "Total neutron-nucleus cross sections at intermediate energies," *Nucl. Phys. A*, vol. 490 (1988). EXFOR 22117(891007C).

23. J. Petler, M. Islam, R. Finlay, and F. Dietrich, "Microscopic optical model analysis of nucleon scattering from light nuclei," *Phys. Rev. C*, vol. 32 (1985). EXFOR 12973(870107C).

24. N. Olsson, B. Trostell, E. Ramstroem, and B. Holmqvist, "Microscopic and conventional optical model analysis of neutron elastic scattering at 21.6 MeV over a wide mass range," *Nucl. Phys. A*, vol. 472 (1987). EXFOR 22048(871013C).

25. T. Stuart, J. Anderson, and C. Wong, "Elastic scattering of 24-MeV neutrons by Al, Fe, Sn, Bi," *Phys. Rev.*, vol. 125 (1962). EXFOR 11490(760715T).

26. A. Bratenahl, S. Fernbach, R. Hildebrand, C. Leith, and B. Moyer, "Elastic scattering of 84-MeV neutrons," *Phys. Rev.*, vol. 77 (1950). EXFOR 11472(760715T).

27. B. Ragent, "The variation of high-energy total neutron cross sections with energy," vol. 53 (1953). EXFOR 11338(761014T).

28. J. Albergotti and J. Ferguson, "Total neutron cross sections of Cu, Fe, Mg and Al near 14 MeV," *Nucl. Phys.*, vol. 82 (1966). EXFOR 11467(761016T).

29. C. Zanelli, F. Brady, J. Romero, C. Castaneda, and D. Johnson, "Neutron total cross sections of Ca and Fe at 35.3, 40.3 and 50.4 MeV," *Phys. Rev. C*, vol. 33 (1986). EXFOR 12916(850611C).

30. A. Smith, "Neutron scattering and models: iron," *Nucl. Phys. A*, vol. 605 (1996). EXFOR 13606(951129C).

31. S. El-kadi, C. Nelson, F. Purser, R. Walter, A. Beyerle, C. Gould, and L. Seagondollar, "Elastic and inelastic scattering of neutrons from 54-,56-Fe and 63-,65-Cu (part I)," *Nucl. Phys. A*, vol. 390 (1982). EXFOR 10958(830526C).

32. S. Mellema, R. Finlay, F. Dietrich, and F. Petrovich, "Microscopic and conventional optical model analysis of fast neutron scattering from Fe-54,56," *Phys. Rev. C*, vol. 28 (1983). EXFOR 12862(840426C).

33. R. Pedroni, C. Howell, G. Honore, H. Pfutzner, R. Byrd, R. Walter, and J. Delaroche, "Energy dependence of the deformed optical potential for neutron scattering from 54,56Fe and 58,60Ni up to 80 MeV," *Phys. Rev. C*, vol. 38 (1988). EXFOR 12997(870220C).

34. R. Finlay, W. Abfalterer, G. Fink, E. Montei, T. Adami, P. Lisowski, G. Morgan, and R. Haight, "Neutron total cross sections at intermediate energies," *Phys. Rev. C*, vol. 47 (1993). EXFOR 13569(930212C).

35. S. Tanaka and Y. Yamanouti, "Fast neutron scattering from Zr-90 and Zr-92," (1980). EXFOR 21638(800825C).

36. Y. Wang and J. Rapaport, "Neutron scattering from 90,91,92,94Zr," *Nucl. Phys. A*, vol. 517 (1990). EXFOR 13160(890509C).

37. D. Bainum, R. Finlay, J. Rapaport, M. Hadizadeh, and J. Carlson, "Isospin effects in nucleon inelastic scattering from single-closed-shell nuclei. (i).the n=50 isotones," *Nucl. Phys. A*, vol. 311 (1978). EXFOR 10729(790319C).

38. R. Clarke and W. Cross, "Elastic and inelastic scattering of 14.1 MeV neutrons from Ni and Zr," *Nucl. Phys. A*, vol. 95 (1967). EXFOR 11768(760731T).

39. J. Rapaport, T. Cheema, D. Bainum, R. Finlay, and J. Carlson, "Neutron scattering from Pb-208," *Nucl. Phys. A*, vol. 296 (1978). EXFOR 10871(790426C).

40. R. Finlay, J. Annand, T. Cheema, J. Rapaport, and F. Dietrich, "Energy dependence of neutron scattering from 208-Pb in the energy range 7-50 MeV," *Phys. Rev. C*, vol. 30 (1984). EXFOR 12865(840426C).

41. R. Vito, "Determination of the coulomb correction and isovector terms of the nucleon-nucleus optical model potential from neutron elastic scattering at 30.3 and 40 MeV," *Diss. Abstr. B*, vol. 40 (1980). EXFOR 12701(811110C).

42. W. Mcgill, R. Carlson, T. Short, J. Cameron, J. Richardson, I. Slaus, W. Oers, J. Verba, D. Margaziotis, and P. Doherty, "Measurements of the proton total reaction cross section for light nuclei between 20 and 48 MeV," *Phys. Rev. C*, vol. 10 (1974). EXFOR O0325(970403C).

43. P. Kirkby and W. Link, "Faraday-cup measurement of proton total reaction cross sections at 100 MeV," *Can. J. Phys.*, vol. 44 (1966). EXFOR O0340(970606C).

44. R. Pollock and G. Schrank, "Proton total reaction cross sections at 16.4 MeV," *Phys. Rev. B*, vol. 140 (1965). EXFOR O0368(970702C).

45. B. Ridley and J. Turner, "Optical model studies of protons scattering at 30 MeV. differintial cross sections for elastic scattering of protons at 30.3 MeV," *Nucl. Phys.*, vol. 58 (1964). EXFOR O0142(950626C).

46. H. Ohnuma, B. Brown, D. Dehnhard, K. Furukawa, T. Hasegawa, S. Hayakawa, N. Hoshino, K. Ieki, M. Kabasawa, K. Maeda, K, Miura, K. Muto, T. Nakagawa, K. Nisimura, H. Orihara, T. Suehito, T. Tohei, and M. Yasue, "A comparative study of the 13c(p,p)13C and 13c(p,n)13N reactions at Ep=35MeV," *Nucl. Phys. A*, vol. 456 (1986). EXFOR E0145(900913T).

47. J. Fannon, E. Burge, D. Smith, and N. Ganguly, "Elastic and inelastic scattering of 50 MeV protons by C-12 and O-16," *Nucl. Phys. A*, vol. 97 (1967). EXFOR O0056(941104C).

48. R. Carlson, A. Cox, J. Nimmo, N. Davison, S. Elbakr, J. Horton, A. Houdayer, A. Sourkes, W. Oers, and D. Margaziotis, "Proton total reaction cross sections for the doubly magic nuclei O-16,Ca-40 and Pb-208 in the energy range 20-50 MeV," *Phys. Rev. C*, vol. 12 (1975). EXFOR O0330(970415C).

49. J. Cameron, J. Richerdson, W. Oers, and J. Verba, "Studies of the energy dependence of p-O-16 interactions between 20 and 50 MeV measurements of the differential cross section of protons elastically scattered by O-16 at 23.4,24.5,27.3,30.1,34.1,36.8,39.7,43.1 and 46.1 MeV," *Phys. Rev.*, vol. 167 (1968). EXFOR O0059(941108C).

50. H. Ohnuma, N. Hoshino, K. Ieki, M. Iwase, H. Shimizu, H. Toyokawa, T. Hasegawa, K. Nisimura, M. Yasue, H. Kabasawa, T. Nakagawa, T. Tohei, H. Orihara, S. Hayakawa, K. Miura, T. Suehiro, S. Nanda, D. Dehnhard, and M. Franey, "The O-16(p,p) reaction at 35 MeV," *Nucl. Phys. A*, vol. 514 (1990). EXFOR O0061(941110C).

51. H. Sakaguchi, M. Nakamura, K. Hatanaka, A. Goto, T. Noro, F. Ohtani, H. Sakamoto, H. Ogawa, and S. Kobayashi, "Elastic scattering of 65 MeV polarized protons," *Phys. Rev. C*, vol. 26 (1982). EXFOR O0032(941020C).

52. J. Menet, E. Gross, J. Malanify, and A. Zucker, "Total-reaction-cross section measurements for 30-60-MeV protons and the imaginary optical potential," *Phys. Rev. C*, vol. 4 (1971). EXFOR O0081(950221C).

53. P. Renberg, D. Measday, M. Pepin, P. Schwaller, B. Favier, and C. Richard-serre, "Reaction cross sections for protons in the energy range 220-570 MeV," *Nucl. Phys. A*, vol. 183 (1972). EXFOR O0213(960523C).

54. I. Dayton and G. Schrank, "Elastic scattering of 17-MeV protons by nuclei," *Phys. Rev.*, vol. 101 (1956). EXFOR O0262(961029C).

55. F. Bertrand and R. Peelle, "Tabulated cross sections for hydrogen and helium particles produced by 62 MeV and 29 MeV protons on 27-Al," Tech. Rep. ORNL-4455, Oak Ridge National Lab., Tenn (1969). EXFOR O0292(940927C).

56. A. Taylor and E. Wood, "Proton scattering from light elements at 142 MeV," *Nucl. Phys.*, vol. 25 (1961). EXFOR O0247(960924C).

57. R. Mccamis, N. Davison, W. Oers, R. Carlson, and A. Cox, "A study of proton total reaction cross sectoins for several medium-mass nuclei between 20 and 48 MeV," *Can. J. Phys.*, vol. 64 (1986). EXFOR O0057(941104C).

58. S. Eccles, H. Lutz, and V. Madsen, "Study of the strongly excited 2+ and 3- states in the Fe-54,56 and Ni-58,60,62 isotopes by proton scattering at 18.6 and 19.1 MeV," *Phys. Rev.*, vol. 141 (1966). EXFOR O0167(950706C).

59. V. Comparat, R. Frascaria, N. Marty, M. Morlet, and A. Willis, "Proton-nucleus elastic scattering at 156 MeV," *Nucl. Phys. A*, vol. 221 (1974). EXFOR O0049(941101C).

60. W. Makofske, G. Greenlees, H. Liers, and G. Pyle, "Proton elastic scattering measurements at 16 MeV with optical-model analysis," *Phys. Rev. C*, vol. 5 (1972). EXFOR O0391(970701C).

61. L. Blumberg, E. Gross, A. Woude, A. Zucker, and R. Bassel, "Polarizations and differential cross sections for the elastic scattering of 40-MeV protons from C-12,Ca-40, Ni-58,Zr-90 and Pb-208," *Phys. Rev.*, vol. 147 (1966). EXFOR O0208(960506C).

62. A. Nadasen, P. Schwandt, P. Singh, W. Jacobs, A. Bacher, P. Debevec, M. Kaitchuck, and J. Meek, "-elastic scattering of 80 - 180 MeV protons and the proton-nucleus optical potential," *Phys. Rev. C*, vol. 23 (1981). EXFOR O0301(941004C).

63. E. Hagberg, A. Ingemarsson, and B. Sundqvist, "Scattering of 185 MeV protons from Zr-90," *Physica Scripta*, vol. 3 (1971). EXFOR O0351(970608C).

64. W. Oers, H. Haw, N. Davison, A. Ingemarsson, B. Fagerstroem, and G. Tibell, "-optical-model analysis of p+208-Pb elastic scattering from 15 - 1000 MeV," *Phys. Rev. C*, vol. 10 (1974). EXFOR O0287(941004C).

65. C. Fulmer, J. Ball, A. Scott, and M. Whiten, "Elastic scattering of 61.4-MeV protons," *Phys. Rev.*, vol. 181 (1969). EXFOR O0211(960514C).

66. Y. Lee, "ECISPLOT: An Interactive Optical Model Parameter Searcher with Simulated Annealing Algorithm," Tech. Rep. NDL-9/99, KAERI (1999).

67. J. Raynal, "Notes on ECIS94," Tech. Rep. CEA-N-2772, Commisariat á l'Energie Atomique (CEA), Saclay, France (1994).

68. F. Goffe, R. H., and A. R. Musgrove, "Global Optimization of Statistical Functions with Simulated Annealing," *J. of Econometrics*, vol. 60, pp. 65–100 (1994).